

Numerical Simulation and Experimental Investigation of the Lift-off and Blowout of Enclosed Laminar Flames

Rajasekhar Venuturumilli, Yong Zhang and Lea-Der Chen

Department of Mechanical and Industrial Engineering, and

National Advanced Driving Simulator

The University of Iowa

Iowa City, IA 52242

INTRODUCTION

Enclosed flames are found in many industrial applications such as power plants, gas-turbine combustors and jet engine afterburners. A better understanding of the burner stability limits can lead to development of combustion systems that extend the lean and rich limits of combustor operations. This paper reports a fundamental study of the stability limits of co-flow laminar jet diffusion flames. A numerical study was conducted that used an adaptive mesh refinement scheme in the calculation. Experiments were conducted in two test rigs with two different fuels and diluted with three inert species. The numerical stability limits were compared with microgravity experimental data. Additional normal-gravity experimental results were also presented.

NUMERICAL

An adaptive mesh refinement (AMR) is used to replace the single-grid numerical scheme of Sheu and Chen (1996). Based on user-defined criteria, the AMR forms successive fine grids on a base coarse grid in a sequential order, e.g., see Berger and Oliger (1984), Almgren et al. (1998) and Pember et al. (1998). A finite volume is used to discretize the computational domain into a staggered, non-uniform grid mesh. A semi-implicit fractional step time marching scheme is used to solve the transport equations of mass, momentum, energy and species. The major assumptions are axisymmetric, low Mach-number laminar flow, Newtonian fluid, negligible viscous dissipation and no radiative heat loss. A four-step reduced mechanism is used to model the methane oxidation. The reduced mechanism is based on an extended Peters mechanism (Sheu, 1996) that incorporates a fifty-step starting mechanism and considers seventeen species. The mechanism invokes steady-state approximations for ten species, i.e., O, OH, C, CH, CH₂, CH₃, CHO, CH₂O, HO₂ and H₂O₂, and solves seven reactive species, i.e., CH₄, H, H₂, H₂O, CO, CO₂ and O₂. A more detailed description of the numerical scheme is given in Venuturumilli and Chen (2003).

EXPERIMENTAL

Two test rigs were used to determine the stability limits of enclosed laminar flames. The laminar flames were fueled by methane or ethane with diluent gases of N₂, He or Ar. The dilution was used to yield the same fuel mass fractions as the baseline case of CH₄/N₂ (50% by volume). The fuel mixtures have the same stoichiometric mixture fraction values. One of the test rigs is the NASA's ELF rig. The ELF has an inner cross-section of 90 mm by 90 mm and an axial length of 150 mm. A fuel tube of 1.6 mm in diameter is used. The second test rig is the

NASA's MAGIC rig, which has an inner cross-section of 100 mm by 100 mm and an axial length of 400 mm. A 12-mm fuel tube is used.

RESULTS AND DISCUSSION

Numerical. The AMR code was validated by comparing the results with published calculations of an axisymmetric, Burke-Schumann diffusion flame (Sheu and Chen, 1996). The AMR code is also used to calculate the stability limits of an experimental flame. The experimental flame was the ELF Glovebox Investigation, on-board of the NASA STS-87/USMP-4 Space Shuttle Mission. A single-grid was used in earlier efforts to calculate the ELF stability limits. The grid resolutions that we had attempted, however, were not adequate; the calculations resulted in unacceptable numerical diffusion errors that falsely stabilized the flame at high fuel jet velocity conditions. Further "static" grid refinements of the flow field were not pursued as computational efforts were already excessive for the grid resolutions examined. Instead, the current AMR code was developed and used. Comparison of the single-grid and AMR calculations was summarized in Fig. 1. As can be seen in Fig. 1, the AMR code yielded converged results without the false stabilization effects. The stability limits calculated by the AMR were compared, in qualitative agreement, with the experimental results.

The AMR code was also used to study the structures of the laminar flames at the attached, lifted and near-blowout conditions. The contours of the local heat release rates are plotted in Fig. 2 for the fuel jet velocity at 0.2 m/s and air flow velocities of 0.1 (attached), 0.3 (lifted), or 0.6 (near blowout) m/s. The heat release rates in the mixture fraction space are shown in Fig. 3. The heat release rates reach their maximum near the stoichiometric locations for the attached and lifted flames. For the near blowout conditions, the maximum, however, occurs on the lean side in the mixture fraction space. The maximum values for all three cases are nearly the same. For the flame stabilized slightly above the burner exit (fuel at 0.2 m/s and air at 0.3 m/s), there is a second local maximum on the lean side as shown in Fig. 4. The corresponding scalar dissipation rates are shown in Fig. 5. The profiles of the scalar dissipation rates are qualitatively similar to those of the heat release rates, cf. Figs. 4 and 5. The peak heat release rates and scalar dissipation rates are not located at the stoichiometric surface for the near blowout conditions. They are located at the lean side of the stoichiometric location. Although Fig. 2 showed a "triple-flame" like picture near the flame base (or the edge flame), no apparent triple flame characteristics are observed when the results are plotted in the mixture fraction space.

Experimental. The stability results shown in Fig. 6 included the results of the baseline case (CH₄/N₂), and the mixtures of CH₄/Ar and C₂H₆/N₂. These mixtures had the same fuel mass fractions as the baseline case; the respective fuel mole fractions were 0.59 and 0.37. A CH₄/He mixture (with the fuel mass fraction same as the baseline case) was also used. However, a stable, lifted flame was not observed for this CH₄/He mixture. Over the conditions examined, the CH₄/Ar flame was more stable than the CH₄/N₂ flame. The C₂H₆/N₂ flame was more stable than the CH₄/Ar flame. The difference of the coflowing air velocities between the CH₄/Ar and CH₄/N₂ flames at lifted and blowout conditions was 0.18 m/s. The standard deviation was 0.004 m/s. It is noted that the fuel mixtures in Fig. 6 have the same stoichiometric mixture fraction values. The binary diffusion coefficients (D) of fuel or inert species (for diffusion into the mixture), however, are different. The adiabatic flame temperatures calculated using the NASA equilibrium code, McBride et al. (1993), are 1810K, 2124 K, 2180 K and 2152 K for the

mixtures of CH₄/He, CH₄/N₂, CH₄/Ar and C₂H₆/N₂, respectively. The substantially lower adiabatic flame temperature of the CH₄/He-air flame probably is an important factor that may have led to the blowout of the flame once it lifted from the burner. The calculated adiabatic flame temperatures and reported maximum laminar burning velocities of CH₄- and C₂H₆-air flames are similar. The C₂H₆/N₂ flame requires higher coflowing air velocities to reach the liftoff and blowout conditions at given fuel jet velocities. It is noted that C₂H₆ species has a lower binary diffusion coefficient than CH₄. The stability limits of CH₄/Ar, CH₄/N₂ and CH₄/He mixtures are also in qualitative agreement with the trend of $D_{Ar} < D_{N_2} < D_{He}$, where D is the binary diffusion coefficient. These observations suggest that species diffusion might also be an important factor in the stability limits of co-flow laminar diffusion flames.

The stability limits of CH₄/N₂ diffusion flames in ELF and MAGIC test rigs are summarized in Fig. 6. The test results showed that there was a distinct transition from a lifted flame to the blowout when tests were conducted using the ELF rig in normal gravity. However, this transition was not observed when the experiments were conducted in the MAGIC rig. The distinct transition from a lifted flame to the blowout condition was in agreement with Papanikolaou and Wierzba (1996), in which a critical coflowing air velocity of 0.3 m/s was reported for a burner diameter of 1.5 mm, and no stable lifted flames were observed when the coflowing air velocity was increased beyond this critical value. The coflowing air velocities of ELF liftoff conditions are lower than the critical velocity of 0.3 m/s, and stable lifted flames are observed. The burner diameter used in the MAGIC rig (12 mm) is larger than the maximum diameter (2 mm) used by Papanikolaou and Wierzba (1996). Direct comparison with their results was not made in current study. Further study is needed to gain additional insight on the effects of the fuel jet nozzle size, diluent gases and transport properties on the stability limits.

ACKNOWLEDGMENT

This work is supported, in part, by NASA Office of Biological and Physical Research, Grant No. NCC3-666, under the management of M.K. King.

REFERENCES

- Almgren, A. S., Bell, J. B., Collella, P., Howell, L. H. and Welcome, M. L., , J. Comput. Phys., 142 (1): 1-46 (1998).
- Berger, M. J., and Olinger, J.. J. of Comput. Phys., 53 (3): 484-512 (1984).
- McBride, B. J., Gordon, S. and Reno, M. A., NASA Technical Memorandum 4513, (1993).
- Papanikolaou and Wierzba (1996), ASME J. Energy Res. Tech., 118 (2): 134-139 (1996).
- Pember, R. B., Howell, L. H., Bell, J. B., Colella, P., Crutchfield, W. Y., Fiveland, W. A. and Jessee, J. P., Combust. Sci. and Tech., Vol. 140, pp. 123-168 (1998).
- Sheu, J.-C. and Chen, L.-D., AIAA J., Vol. 34, No. 10, pp. 2090-2098 (1996).
- Sheu, J.C., "Numerical Simulation of Burke-Schumann Diffusion Flame Using Finite-Rate Chemical Kinetics," Ph. D. Dissertation, The University of Iowa, Iowa City, Iowa (1996).
- Venuturumilli, R. and Chen, L.-D., AIAA Paper No. 2003-0807, AIAA (2003).

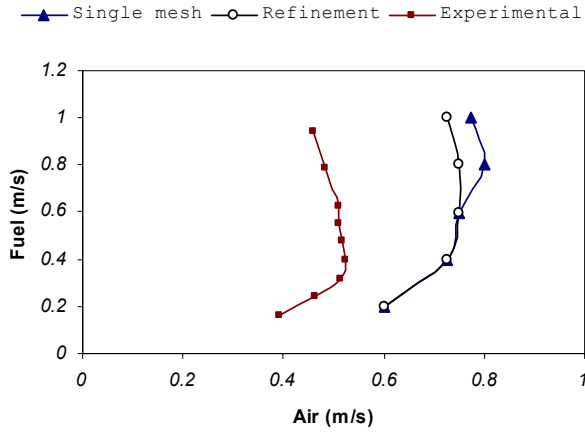


Figure 1. Comparison with experimental data of blowout conditions in 0g.

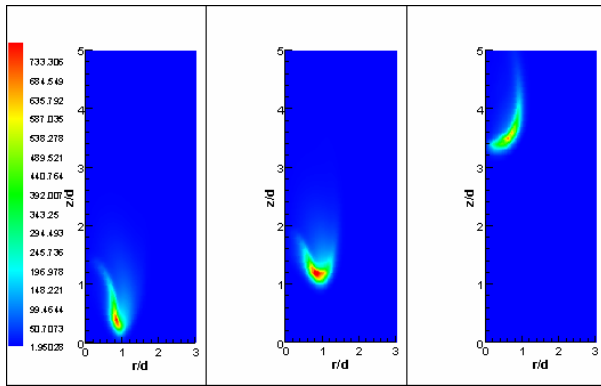


Figure 2. Heat release rate contours, fuel at 0.2 m/s and air at 0.1 m/s, 0.3 m/s or 0.6 m/s.

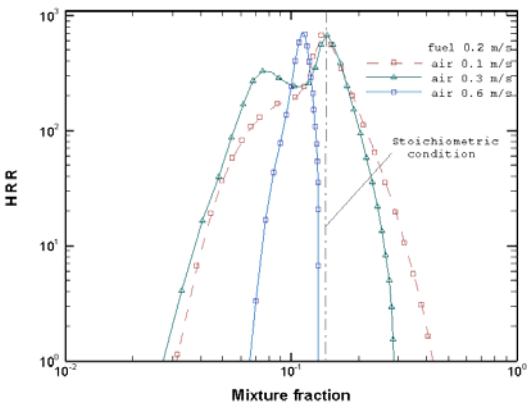


Figure 3. The heat release rates of attached (air at 0.1 m/s), lifted (air at 0.3 m/s) and near blowout (air at 0.6 m/s) flames.

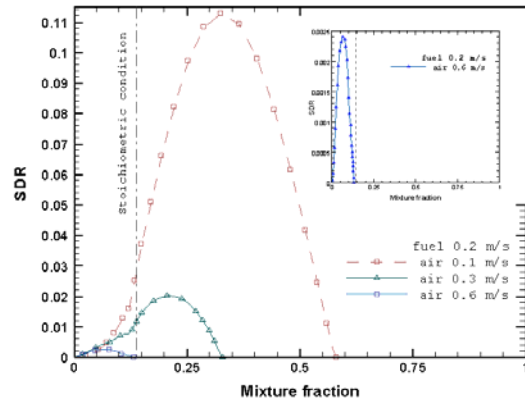


Figure 4. The heat release of attached (air at 0.1 m/s) and lifted (air at 0.3 m/s) flames.

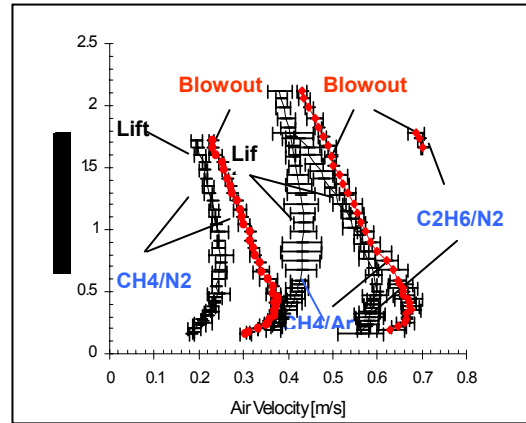


Figure 5. Summary of ELF stability results.

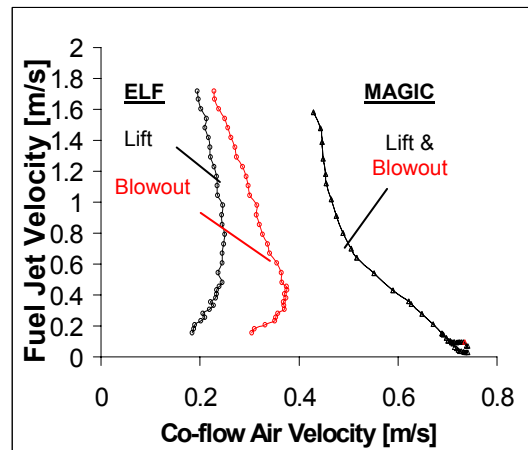


Figure 6. Summary of ELF and MAGIC CH4/N2 stability results.